Analyst

RSC Publishing

PAPER

View Article Online
View Journal | View Issue

# A novel label-free electrochemical microRNA biosensor using Pd nanoparticles as enhancer and linker

Cite this: *Analyst*, 2013, **138**, 1060

Xiaoyan Wu, Yaqin Chai,* Ruo Yuan,* Huilan Su and Jing Han

In this paper, a novel, label-free amperometric biosensor for the detection of microRNA-155 based on the conductive self-assembled multilayer comprised of Nafion, thionine (Thi) and Pd nanoparticles was successfully prepared. Nafion was firstly dropped on to a bare glass carbon electrode. Then Thi was absorbed by the cation exchanger Nafion. Furthermore, a Pd nanoparticles layer which was used to immobilize target biomolecules was constructed by the amino group of Thi as linker. Moreover, the proposed biosensor showed excellent electrocatalytic activity towards $H_2O_2$ and enhanced the current response of the biosensor. Cyclic voltammetry was used for the characterization and electrochemical properties of the stepwise self-assembly process of the biosensor, and scanning electron microscopy was used for observing the microstructure of the modified film. Using microRNA-155 as a model, the resulting biosensor presented high sensitivity, good stability and a broad linear response from 5.6 to 5.6 $\times 10^5$ pM with the detection limit of 1.87 pM under optimization of the assay conditions.

Received 17th October 2012
Accepted 11th December 2012

DOI: 10.1039/c2an36506e

www.rsc.org/analyst



## Introduction

MicroRNAs (miRNAs) are short, approximately 19–23 nucleotides long, endogenous, non-coding, single-stranded RNAs that can regulate the expression of genes at both the translational and transcriptional levels.[1–5] They are also key post-transcriptional regulators of gene expression during both normal and transformative biological processes, including stem cell differentiation, apoptosis, proliferation, motility, invasiveness, disease development and tumorigenesis.[6,7] Recently, over 900 unique human miRNA sequences have been published in the miRBase database, and almost 346 records among them correlate to all kinds of human diseases.[8] Almost 30% of coding protein genes are regulated up by miRNAs and the number of genes modulated by miRNAs has increased sharply.[9] An abnormal miRNA may produce a series of consecutive pathological changes. In recent years, many studies have demonstrated that the expression of miRNA was either up-regulated or down-regulated in human cancer.[10] Acting as oncogenes or tumor suppressors, deregulated miRNAs expressed aberrantly may affect tumorigenesis and lead to malignant transformation.[6,11] So many abnormal miRNAs are correlated with numerous cancers, which are the leading cause of disease-related deaths in the world. For example, miR-222 and miR-221 are often up-regulated in papillary carcinoma.[12] High levels of miR-21 are associated with breast cancer.[13] Owing to the fairly informative miRNA profiles which reflect the developmental lineage and differentiation state of tumors, the practical implication of miRNAs can serve as an early warning signal and represent a potential therapeutic target as well as a prognostic biomarker for the diagnosis of human cancers.[3,14] Therefore, developing a sensitive, rapid and quantitative detection method for miRNAs comes into prominence.

In this work, we choose miRNA-155, whose expression is consistently involved in a wide range of diseases and pathogenesis including oncogenesis, as the subject of the study. Currently, we know that miRNA-155 is overexpressed or mutated in various malignant tumor cells, such as hepatocellular carcinoma (HCC),[15,16] non-small cell lung cancer (NSCLC),[8] breast cancer,[17] colon cancer,[18] chronic lymphocytic leukemia (CLL),[3] *etc*. Also, it has been demonstrated that miRNA-155 plays a key role in the mammalian immune system.[19] Generally speaking, miRNA-155 treated as a biomarker in certain types of cancer is reasonable and effective. Discovering a rapid, accurate, sensitive and quantitative method to detect miRNA-155 is imperative and meaningful work.

However, the detection of the small miRNAs is confronted by many problems. The extremely short size of the miRNA has presented great challenges for developing ultrasensitive and *in-situ* assays.[20] Based on hybridization, traditional molecular biology techniques for miRNA detection, such as cloning and northern blotting assays, are time-consuming and not very sensitive.[7,21] To enhance the sensitivity of the miRNA assay, reverse-transcriptase polymerase chain reaction (RT-PCR) approaches flourished because of their exceptional amplification by extending sequences constantly and repeatedly. However, the PCR-based methods required the use of small

*Education Ministry Key Laboratory on Luminescence and Real-Time Analysis, College of Chemistry and Chemical Engineering, Southwest University, Chongqing 400715, People's Republic of China. E-mail: yuanruo@swu.edu.cn; Fax: +86-23-68253172; Tel: +86-23-68252277*

primers, otherwise running too many replicates for miRNAs was not feasible and not cost-effective.[22] During the last decade, several new detection methods based on optical and electronic signal transduction have emerged.[23,24] Quantitative determination of miRNAs by electrochemical methods was based on changes in circuit properties such as capacitance, conductance and resistance that occur before and after target miRNA hybridization.[25] Gao and Yu developed a miRNA biosensor, but the method needed to bind $Os(dmpy)_2(IN)Cl^+$ on such small miRNA templates, which made the process time-consuming and difficult.[26] Kilic *et al.* made an electrochemical detection based on the enzyme-amplified biosensing of miRNA-21 and achieved a detection level of 6 pM.[27] Although sensitive, the approaches mentioned above were complicated. Meanwhile, electrochemical biosensors for detecting miRNA based on changes of current response were rare. In view of miRNAs detection with higher sensitivity and better reliability, nanoscale materials possessing electronic properties have been widely used to gain prominent performance for miRNA detection devices, especially metal nanoparticles. Numerous metal nanoparticles with distinguishing characteristics were reported, such Pt and Au nanoparticles.[28,29] Owing to their well-known biocompatibility and satisfactory conductivity, Pd nanoparticles (nano-Pd) have received increasing applications in biosensor systems. What is more, nano-Pd was usually used as a catalyst due to its excellent electrocatalytic activity for hydrogen peroxide ($H_2O_2$).[30] Additionally, nano-Pd could be employed as a linker for the immobilization of biomolecules.[31] Thus, we designed a novel, label-free biosensor for miRNA-155 detection based on changes of current response with the unique combination of Nafion, thionine (Thi) and nano-Pd. Nafion was employed to form a stable and uniform film on the surface of a glassy carbon electrode (GCE). Then, Thi could be absorbed on the Nafion film by electronic exchange function. Furthermore, nano-Pd was immobilized on the modified electrode surface through the interaction between nano-Pd and the amino group of Thi. Herein, nano-Pd effectively catalyzed $H_2O_2$ and significantly enhanced the detectability of miRNA. Simultaneously, the conjunction between nano-Pd and thiols modified of the primer was also used for the immobilization of primers. In this case, nano-Pd played a crucial role in the fabrication of the biosensor, especially in amplifying the sensitivity and lowering the detection limit. The proposed biosensor for detecting miRNA-155 presented high sensitivity, assay simplicity, remarkable stability and good reproducibility.

## Experimental

### Chemicals and material

All synthetic oligonucleotides were purchased from TaKaRa (Dalian. China), and were kept at 4 °C before use. MiRNA-155 primer was modified a free thiol at its 5′ terminus for immobilization on the electrode surface. The base pair sequences of the miRNA-155 primer and miRNA-155 oligonucleotides are listed in Table 1. The sequences of the thrombin aptamer (TBA) and PDGF binding aptamer (PBA) were as follows:

TBA: 5′-GGT TGG TGT GGT TGG-3′;

PBA: 5′-CAG GCT ACG GCA CGT AGA GCA TCA CCA TGA TCC TG-3′.

Potassium palladium(II) chloride ($K_2PdCl_4$), sodium borohydride ($NaBH_4$), hexanethiol (HT), Nafion and Thi were obtained from Sigma Chemical Co. (St Louis, MO, USA). Hydrogen peroxide ($H_2O_2$, 30%, w/v solution) was purchased from Chemical Reagent Co. (Chongqing, China). All chemicals and solvents were of analytical grade and were used as received. Double distilled water was used throughout this study. The acetate buffer solution (pH 5.5) was prepared with 0.1 M HAc–NaAc containing 0.1 M KCl. Buffer for dispersing the Pd nanoparticles was phosphate buffered solution (PBS, pH 7.4), prepared by mixing the solutions of $Na_2HPO_4$, $KH_2PO_4$ and KCl. Buffer for preparation of miRNA-155 solutions was 20 mM Tris–HCl containing 140 mM NaCl, 1 mM $MgCl_2$, 5 mM KCl and 1 mM $CaCl_2$, pH 7.4.

### Apparatus

Cyclic voltammetric (CV) measurements were carried out using a CHI 660A electrochemistry workstation (Shanghai CH Instruments, China). A conventional three-compartment electrochemical cell comprised a platinum wire auxiliary electrode, a saturated calomel reference electrode (SCE) and modified GCE ($\varnothing = 4$ mm) as the working electrode. The size of the nanoparticles was estimated by scanning electron microscope (SEM, S-4800, Hitachi, Tokyo, Japan). The pH measurements were performed with a pH meter (MP 230, Mettler-Toledo, Switzerland) and digital ion analyzer (Model PHS-3C, Dazhong Instruments, Shanghai, China).

### Preparation of nano-Pd

Nano-Pd was prepared successfully according to a simple redox method reported previously with slight modifications.[31] Firstly, 2 mL of 10 mM $K_2PdCl_4$ aqueous solution was prepared. Subsequently, under successively vigorous stirring, another 2 mL of 0.1 M $NaBH_4$ was slowly added into the $K_2PdCl_4$ aqueous solution, changing the color of the solution gradually to black. After 2 h of stirring, the products were obtained by centrifugation and were washed with double distilled water three times. Finally, the products were dispersed in 500 μL PBS (pH 7.4) solution, which were stored in a refrigerator at 4 °C when not in use.

### Fabrication of the biosensor for detecting miRNA-155

Prior to surface modification, the GCE with a diameter of 4 mm was polished repeatedly with 0.3 μm and 0.05 μm alumina slurry to obtain a mirror-like surface, followed by successive sonication in double distilled water, anhydrous ethanol and double distilled water each for 5 min and drying in air. Subsequently, 6 μL of 2.5 wt% Nafion was dropped onto the cleaned GCE. After drying at room temperature, the modified electrode was immersed into 3 mM Thi solution for 10 min, and then washed with double distilled water. Next, 10 μL of the previously synthesized nano-Pd dispersion was added onto the electrode surface and washed 2 h later. Following that, the obtained electrode was incubated in 20 μL miRNA-155 primer solution

**Table 1** MiRNA-155 primer and miRNA-155 sequences used in this work

| | |
|---|---|
| MiRNA-155 primer | 5′-HS–AAA AAA AAC CCC UAU CAC GAU UAG CAU UAA-3′ |
| MiRNA-155 | 5′-UUA AUG CUA AUC GUG AUA GGG GU-3′ |

for 16 h at 4 °C. Finally, the proposed electrode was incubated in 20 μL of HT solution (1 mM) for approximately 40 min in order to block the possible remaining active groups and eliminate any non-specific absorption. The prepared biosensor for detecting miRNA-155 was stored at 4 °C when not in use. The schematic diagram of the stepwise fabrication procedure was shown in Scheme 1.

### Experimental measurements

Electrochemical experiments were performed in a standard three-electrode system. The electrochemical characteristics of the prepared biosensor were carried out by CV scanning from −0.5 to 0.1 V (*vs.* SCE) in 3 mL 0.1 M HAc–NaAc buffer (pH 5.5) containing 0.1 M KCl at room temperature with a sweeping rate of 50 mV $s^{-1}$.

The detection was based on the change of the amperometric response before and after the miRNA-155 primer–target recognition reaction. When the background of the biosensor current was stabilized, the peak of the current response was recorded as $I_0$. Then, the miRNA-155 primer–target recognition reaction took place, and after that the peak current which decreased to a minimum, owing to the resulting complex hindering the electron-transfer, was recorded as $I$. Therefore, the change of current response ($\Delta I$) was given by $\Delta I = I_0 - I$. $\Delta I$ was dependent on the degree of the miRNA-155 primer–target recognition reaction, which could be used for the determination of miRNA-155.

## Results and discussion

### SEM images of nano-Pd

In this paper, the synthesized nano-Pd was used for the immobilization of the miRNA-155 primer *via* the conjugation between nano-Pd and thiols modified at its 5′ terminus of the miRNA-155 primer. So the synthesis of nano-Pd was critical. SEM was able to provide valuable data about the real shapes of the nanoparticles. An SEM image of the nano-Pd was shown in Fig. 1A, which exhibited a homogeneous configuration and good dispersion in water, and the average size of the nano-Pd was about 30 nm. Compared with the image of solo nano-Pd, Fig. 1B exhibited that nano-Pd was placed upon a layer of Thi/Nafion membrane.

### Electrochemical characteristics of the biosensor detecting for miRNA-155

CV was a convenient and effective tool for providing electroactivity information concerning different modified electrodes. During the fabrication process, the feature of the stepwise modified electrode surface was investigated by CV in 0.1 M HAc–NaAc buffer solution (pH 5.5), which was shown in Fig. 2. Curve 'a' displayed the CV of a bare GCE. There was no obvious peak displayed (Fig. 2a). After modification with Thi/Nafion, a pair of redox peaks could be observed in curve 'b', which demonstrated that Thi, a material with electrochemical activity, was modified on the electrode surface through opposite-charged absorption by Nafion. Then, it was found that the peak current was decreased with the formation of a nano-Pd monolayer on the modified electrode (Fig. 2c), reflecting that nano-Pd was immobilized successfully through the interaction with the amino groups of Thi. On some occasions, nano-Pd could not be dispersed well and they accumulated together, which made their size slightly larger and induced the little decrease of peak current. The peak current decreased as well when the miRNA-155 primer was immobilized onto the nano-Pd layer (Fig. 2d), which could be attributed to a less conductive membrane formed by the immobilization of the miRNA-155 primer. Subsequently, the modified electrode was blocked with HT, and a further decrease of the peak current was obtained due to the fact that HT could hinder the electron transfer (Fig. 2e). Finally, the peak current was still decreased after the prepared electrode

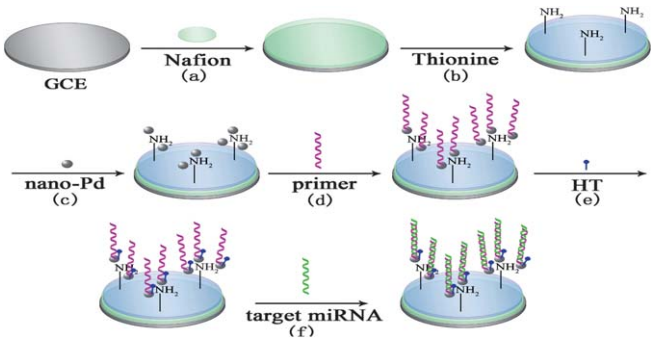


**Scheme 1** Schematic illustration of the stepwise fabrication process of the biosensor for detecting miRNA-155: (a) fabrication of Nafion membrane; (b) absorption of Thi; (c) immobilization of nano-Pd; (d) incubation of miRNA-155 primer; (e) HT blocking.

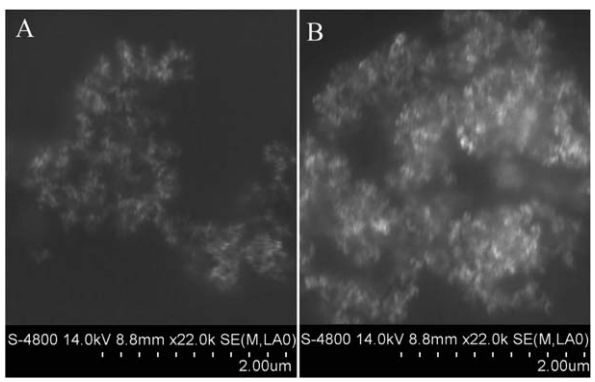


**Fig. 1** SEM images of nano-Pd (A) and nano-Pd/Thi/Nafion (B).

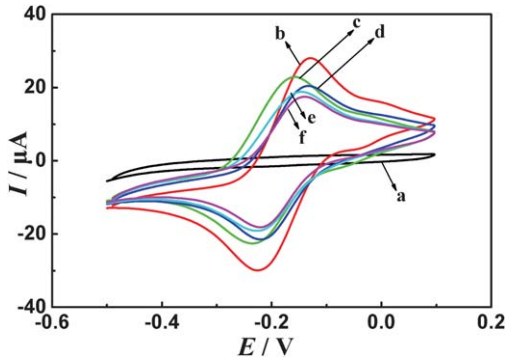


**Fig. 2** CVs in HAc–NaAc buffer solution (pH 5.5) for (a) bare GCE; (b) Thi/Nafion modified GCE; (c) nano-Pd/Thi/Nafion modified GCE; (d) primer/nano-Pd/Thi/Nafion modified GCE; (e) HT/primer/nano-Pd/Thi/Nafion modified GCE; (f) after incubation in the 560 pM miRNA-155 with a scan rate 50 mV $s^{-1}$ and all potentials are given *vs.* SCE.

was incubated with the target (Fig. 2f), 560 pM miRNA-155, indicating that the interaction of combination between the miRNA-155 primer and the target hindered the transmission of electrons towards the electrode surface. The CV measurement demonstrated that the biosensor was very useful for miRNA-155 sensing.

Fig. 3 showed CVs of the modified biosensor in HAc–NaAc buffer solution (pH 5.5) at various scan rates ranging from 20 to 300 mV $s^{-1}$. It was clear that the anodic and cathodic peak currents were dependent on the scan rate. Additionally, peak currents were directly proportional to the scan rates, which exhibited a linear relationship (shown in the inset), indicating a surface-confined redox process.

In order to check on whether or not the immobilized nano-Pd can catalyze $H_2O_2$, $H_2O_2$ was added into 3 mL of the 0.1 M HAc–NaAc buffer solution (pH 5.5). Curves 'a' and 'b' in Fig. 4 showed CVs before and after the addition of 1.8 mM $H_2O_2$, respectively. It could be easily seen that the cathodic peak current increased with the addition of $H_2O_2$, indicating that nano-Pd had impressive electrocatalytic activity for $H_2O_2$. Simultaneously, the amplification of the detection response signals was greatly achieved through the effect of the nano-Pd.

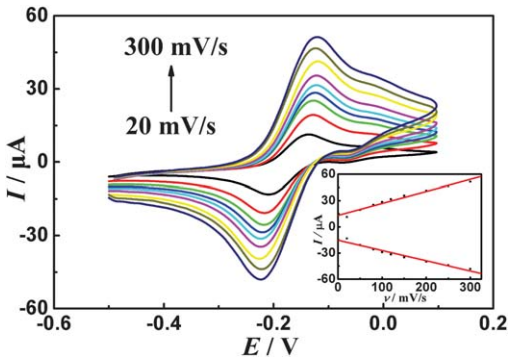


**Fig. 3** CVs of the modified electrode at different scan rates (from inner to outer): 20, 50, 80, 100, 120, 150, 200, 250 and 300 mV $s^{-1}$ in 3 mL HAc–NaAc buffer solution (pH 5.5) at room temperature. All potentials are given *vs.* SCE. The inset shows the dependence of redox peak currents on the potential scan rates.

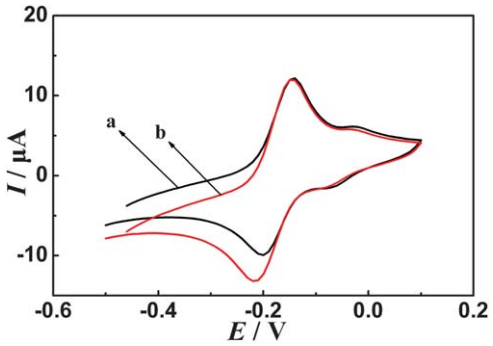


**Fig. 4** CVs of the modified electrode in the HAc–NaAc buffer: (a) without $H_2O_2$; (b) with 1.8 mM $H_2O_2$ at 50 mV $s^{-1}$ scan rate at room temperature. All potentials are given *vs.* SCE.

## Optimization of experimental parameters

The concentration of $H_2O_2$ was connected with the degree of the response signal amplification. In order to acertain which concentration was the most effective one for the biosensor operation, CV measurements were carried out in HAc–NaAc buffer solution (pH 5.5) under successive injections of $H_2O_2$. As shown in Fig. 5A, the cathodic peak current increased with increasing the concentration of $H_2O_2$, indicating a typical electrocatalytic process of $H_2O_2$. However, the cathodic peak current tended to level off after more than 1.8 mM $H_2O_2$ was added. Therefore, 1.8 mM was the optimal concentration of $H_2O_2$ for the experiment.

The influence incubation time on the amperometric response signals of the biosensor for detecting miRNA-155 was also examined. The biosensor was incubated within a 560 pM miRNA-155 solution for 2, 5, 8, 10, 12, 15, 17, 19 and 21 min, and then

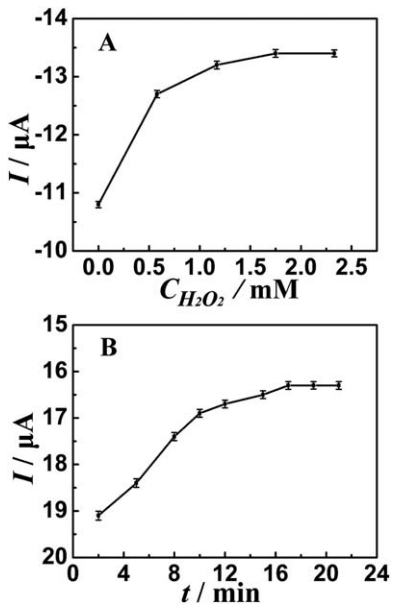


**Fig. 5** (A) Influence of the concentration of $H_2O_2$ on the response signals of the biosensor in the HAc–NaAc buffer solution (pH 5.5) at 50 mV $s^{-1}$ scan rate at room temperature. All potentials are given *vs.* SCE. (B) Influence of incubation time on the response signals of the biosensor. All potentials are given *vs.* SCE.

tested in 3 mL of 0.1 M HAc–NaAc buffer solution (pH 5.5). As shown in Fig. 5B, the peak currents were sharply decreased until the incubation time reached 17 min, and then the amperometric response signals tended to be stable for times greater than 17 min. It meant that an equilibration state of interaction between the miRNA-155 primer and miRNA-155 was reached within 17 min. Therefore, 17 min could be used as the optimal incubation time and was adopted in the subsequent work.

### Performance of the biosensor detecting for miRNA-155

The performance of the present biosensor was evaluated by detecting miRNA-155 standard solution with the CV technique under the optimal assay conditions. The calibration plots were recorded by the peak current response when detecting different concentrations of miRNA-155 (Fig. 6). It was obvious that the peak current of CVs performed decreased with the increasing concentration of miRNA-155. That is, the peak currents were inversely proportional to the concentration of miRNA-155 in working buffer because miRNA-155 acted as a definite barrier for the electron transfer when it was modified on the biosensor surface. The linear range covered from 5.6 to $5.6 \times 10^5$ pM with a regression equation of the form $y = 1.7281x - 1.5025$ and a linear correlation coefficient of 0.9947. A detection limit of 1.87 pM was determined according to a signal to noise ratio of 3. It indicated that the prepared biosensor for detecting miRNA-155 was sensitive and reliable for the determination of miRNA-155 concentrations.

### Stability, repeatability and specificity of the proposed miRNA biosensor

The stability and repeatability were advantages of the designed biosensor for detecting miRNA-155. The repeatability of the biosensor was investigated by the analysis of six equally prepared electrodes which were incubated with same concentration (560 pM) of miRNA-155 (Table 2), and it was found that the relative standard deviation was 0.74% ($n = 6$). The stability was evaluated by 40-continuous cycles in the potential of −0.5 to 0.1 V at the 50 mV $s^{-1}$ scan rate (Fig. 7A), and a relative standard deviation of 4.2% was acquired. In addition, the long-term stability of the biosensor for detecting miRNA-155 was also investigated over a 25-day period (Fig. 7B). The biosensor for detecting miRNA-155 was stored in the refrigerator at 4 °C and was examined intermittently (every 4–7 days). After 25 days, there was no apparent change. Compared with the initial stable response value, less than 10% of the response change was found. Generally speaking, it indicated that the biosensor for detecting miRNA-155 displayed sufficient stability and repeatability.

To test the specificity of the biosensor for miRNA-155 detection, two non-complementary sequences (TBA and PBA) were examined under the same experimental conditions respectively. In the experiment, 5 nM of TBA and 5 nM of PBA were employed to replace 560 pM of miRNA-155. As shown in Fig. 8, it could be found that no significant change of current was observed in comparison with the result obtained in the presence of miRNA-155, indicating that the miRNA biosensor had good specificity towards target miRNA. In addition, the cross-sensitivity of the biosensor in a mixture of three different sequences was also examined. Even though high concentrations of TBA (5 nM) and PBA (5 nM) co-existed in detecting 560 pM of miRNA-155, the $\Delta I$ obtained from the response of the complex had no apparent difference, indicating that TBA and PBA had almost negligible influence on the miRNA-155 detection. These tests showed that our assay was specific for miRNA-155 detection.

**Table 2** Reproducibility assays using repetitive standard of 560 pM miRNA-155 ($n = 6$)

| Electrodes | 1 | 2 | 3 | 4 | 5 | 6 |
|---|---|---|---|---|---|---|
| $I$/μA | 16.4 | 16.2 | 16.2 | 16.1 | 16.3 | 16.4 |

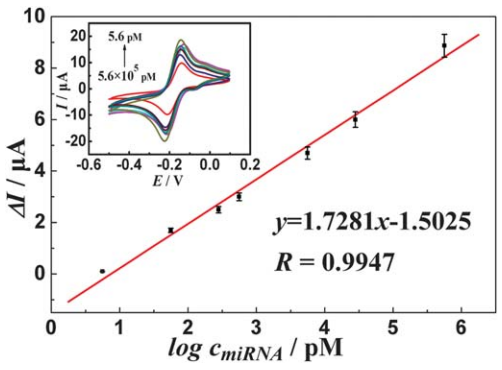


**Fig. 6** Calibration plots of peak current response *vs.* logarithm of concentration of miRNA with the biosensor under optimal conditions. Inset shows the typical CV plots upon the addition of varying amounts of miRNA: 5.6, 56, 280, 560, $5.6 \times 10^3$, $2.8 \times 10^4$, $5.6 \times 10^5$ pM. All potentials are given *vs.* SCE and the scan rate is 50 mV $s^{-1}$.

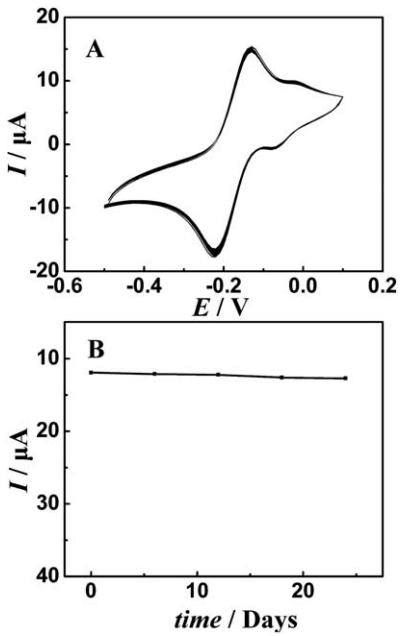


**Fig. 7** (A) 40 cycles of CV measurements in HAc–NaAc buffer solution (pH 5.5) after being incubated in primer. (B): Long-term stability of the biosensor detecting for miRNA-155.

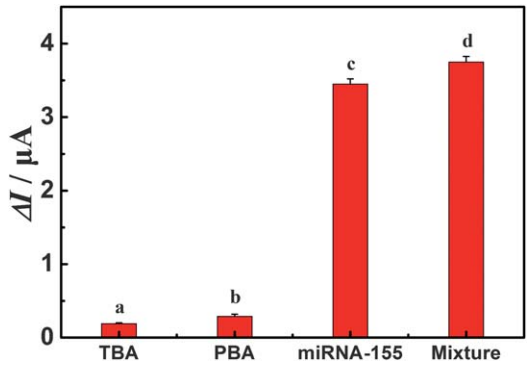


**Fig. 8** Specificity of the miRNA biosensor (a) with 5 nM of TBA; (b) with 5 nM of PBA; (c) with 560 pM of miRNA-155; (d) with 560 pM of miRNA-155 when 5 nM of TBA and 5 nM of PBA co-existed.

**Table 3** Determination of miRNA-155 added in human blood serum ($n = 3$) with the proposed miRNA biosensor

| Sample | Standard value/μA ($I_0$) | Found value/μA ($I$) | Recovery (%) ($I/I_0$) | RSD (%) |
|---|---|---|---|---|
| 1 | 15.83 | 16.07 | 101.52 | 1.65 |
| 2 | 15.52 | 15.55 | 100.19 | 1.25 |
| 3 | 14.42 | 14.35 | 99.51 | 4.40 |
| 4 | 11.87 | 12.62 | 106.32 | 4.76 |
| 5 | 10.81 | 10.37 | 95.93 | 3.93 |

### Analytical application of the miRNA biosensor

To evaluate the applicability of the proposed biosensor, the standard addition method was employed. A series of real samples were prepared by adding different concentrations of miRNA-155 into human blood serum. All experiments were performed in compliance with the relevant laws and institutional guidelines, and the institutional committee had approved the experiments. The analytical results for miRNA-155 were shown in Table 3. From Table 3, we could see that the recovery (between 95.93% and 106.32%) and relative standard deviation (between 1.25% and 4.76%) were acceptable, which indicated that the prepared electrochemical miRNA biosensor had promising analytical applications in real biological samples.

## Conclusions

In summary, a novel amperometric biosensor with high sensitivity, good stability, superior reproducibility and long-term maintenance of bioactivity has been successfully proposed in this study for the determination of miRNA-155, which is based on miRNA-155 primer/nano-Pd/Thi/Nafion. Moreover, the nano-Pd could catalyze $H_2O_2$, which effectively improved the detection sensitivity of the assay. Additionally, we observed that the detection limit of the sensor to miRNA-155 was low and the fabrication process was simple. Accordingly, the proposed sensor was not only suitable for determining miRNA-155 as shown above but also other interesting tumor markers.



## Acknowledgements

The authors are grateful for the National Natural Science Foundation of China (21075100, 21275119), the Ministry of Education of China (Project 708073), Specialized Research Fund of the Doctoral Program of Higher Education (20100182110015) and the Natural Science Foundation Project of Chongqing (CSTC-2009BA1003, CSTC–2010BB4121, CSTC-2011BA7003).

## References

1 Y. Lee, M. Kim, J. Han, K. H. Yeom, S. Lee, S. H. Baek and V. N. Kim, *EMBO J.*, 2004, **23**, 4051.
2 B. R. Cullen, *Mol. Cell*, 2004, **16**, 861.
3 F. Muller, *Mol. Diagn.*, 2010, **10**, 435.
4 K. J. Beezhold, V. Castranova and F. Chen, *Mol. Cancer*, 2010, **9**, 134.
5 M. C. Sempere and I. I. Cáceres, *Clin. Transl. Oncol.*, 2011, **13**, 357.
6 A. J. Qavi, J. T. Kindt and R. C. Bailey, *Anal. Bioanal. Chem.*, 2010, **398**, 2535.
7 T. Donnem, K. Eklo, T. Berg, S. W. Sorbye, K. Lonvik, S. A. Saad, K. A. Shibli, S. Andersen, H. Stenvold, R. M. Bremnes and L. T. Busund, *J. Transl. Med.*, 2011, **9**, 6.
8 M. F. Li, J. Li, X. F. Ding, M. He and S. Y. Cheng, *AAPS J.*, 2010, **12**, 309.
9 B. P. Lewis, C. B. Burge and D. P. Bartel, *Cell*, 2005, **120**, 15.
10 S. Vatolin, K. Navaratne and R. J. Weil, *J. Mol. Biol.*, 2006, **358**, 983.
11 M. L. Yeung and K. T. Jeang, *Pharm. Res.*, 2011, **28**, 3043.
12 M. N. Nikiforova, S. I. Chiosea and Y. E. Nikiforov, *Endocr. Pathol.*, 2009, **20**, 85.
13 K. A. Cissell, Y. Rahimi, S. Shrestha, E. A. Hunt and S. K. Deo, *Anal. Chem.*, 2008, **80**, 2319.
14 J. Lu, G. Getz, E. A. Miska, E. A. Saavedra, J. Lamb, D. Peck, A. S. Cordero, B. L. Ebert, R. H. Mak, A. A. Ferrando, J. R. Downing, T. Jacks, H. R. Horvitz and T. R. Golub, *Nature*, 2005, **435**, 834.
15 Z. B. Han, H. Y. Chen, J. W. Fan, J. Y. Wu, H. M. Tang and Z. H. Peng, *J. Cancer Res. Clin. Oncol.*, 2012, **138**, 153.
16 C. H. Su, Z. H. Hou, C. Zhang, Z. G. Tian and J. Zhang, *Virology J.*, 2011, **8**, 354.
17 W. Kong, L. He, M. Coppola, J. P. Guo, N. N. Esposito, D. Coppola and J. Q. Cheng, *Biol. Chem.*, 2010, **285**, 17869.
18 S. Volinia, G. A. Calin, C. G. Liu, S. Ambs, A. Cimmino, F. Petrocca, R. Visone, M. Iorio, C. Roldo, M. Ferracin, R. L. Prueitt, N. Yanaihara, G. Lanza, A. Scarpa, A. Vecchione, M. Negrini, C. C. Harris and C. M. Croce, *Proc. Natl. Acad. Sci. USA*, 2006, **103**, 2257.
19 T. H. Thai, D. P. Calado, S. Calado, S. Casola, K. M. Ansel, C. C. Xiao, Y. Z. Xue, A. Murphy, D. Frendewey, D. Valenzuela, J. L. Kutok, M. S. Supprian, N. Rajewsky, G. Yancopoulos, A. Rao and K. Rajewsky, *Science*, 2007, **316**, 604.
20 K. A. Cissell, S. Shrestha and S. K. Deo, *Anal. Chem.*, 2009, **79**, 4754.
21 Y. Fan, X. T. Chen, A. D. Trigg, C. H. Tung, J. Kong and Z. Q. Gao, *J. Am. Chem. Soc.*, 2007, **129**, 5437; W. Kong,

L. He, M. Coppola, J. P. Guo, N. N. Esposito, D. Coppola and J. Q. Cheng, *Biol. Chem.*, 2010, **285**, 17869.
22 C. F. Chen, D. A. Ridzon, A. J. Broomer, Z. H. Zhou, D. H. Lee, J. T. Nguyen, M. Barbisin, N. L. Xu, V. R. Mahuvakar, M. R. Andersen, K. Q. Lao, K. J. Livak and K. J. Guegler, *Nucleic Acids Res.*, 2005, **33**, 179.
23 C. Pöhlmann and M. Sprinzl, *Anal. Chem.*, 2010, **82**, 4434.
24 H. Yang, A. Hui, G. Pampalakis, L. Soleymani, F. F. Liu, E. H. Sargent and S. O. Kelley, *Angew Chem., Int. Ed.*, 2009, **48**, 8461.
25 G. J. Zhang, J. H. Chua, R. E. Chee, A. Agarwal and S. M. Wong, *Biosens. Bioelectron.*, 2009, **24**, 2504.
26 Z. Q Gao and Y. H. Yu, *Sens. Actuators, B*, 2007, **121**, 552.
27 T. Kilic, S. N. Topkaya, D. O. Ariksoysal, M. Ozsoz, P. Ballar, Y. Erac and O. Gozen, *Biosens. Bioelectron.*, 2012, **38**, 195.
28 Y. Wang, R. Yuan, Y. Q. Chai, Y. L. Yuan, L. J. Bai and Y. H. Liao, *Biosens. Bioelectron.*, 2011, **30**, 61.
29 Y. Zhuo, P. X. Yuan, R. Yuan, Y. Q. Chai and C. L. Hong, *Biomaterials*, 2009, **30**, 2284.
30 L. Meng, J. Jin, G. X. Yang, T. H. Lu, H. Zhang and C. X. Cai, *Anal. Chem.*, 2009, **81**, 7271.
31 H. Niu, R. Yuan, Y. Q. Chai, L. Mao, Y. L. Yuan, Y. L. Cao and Y. Zhuo, *Chem. Commun.*, 2011, **47**, 8397.